# Vibrational Spectroscopic and ab Initio Studies on Conformations of the Chemical Species in a Reaction of Aqueous 2-(*N*,*N*-Dimethylamino)ethanol Solutions with Carbon Dioxide. Importance of Strong $NH^+\cdots O$ Hydrogen Bonding

**Keiichi Ohno,* Hisashi Matsumoto, Hiroshi Yoshida, and Hiroatsu Matsuura**

*Department of Chemistry, Faculty of Science, Hiroshima University, Kagamiyama, Higashi-Hiroshima 739-8526, Japan*

**Toru Iwaki**

*Hiroshima Research & Development Center, Mitsubishi Heavy Industries, Ltd., Kan-on-shin-machi, Nishi-ku, Hiroshima 733-8601, Japan*

**Taiichiro Suda**

*Plant Siting and Environmental, The Kansai Electric Power Co., Inc., Nakanoshima, Kita-ku, Osaka 530-8270, Japan*

*Received: June 9, 1998; In Final Form: August 7, 1998*

The process of a reaction of aqueous 2-(*N*,*N*-dimethylamino)ethanol (DMAE) solutions with carbon dioxide and the conformations of the chemical species present in the reaction system have been studied by infrared and Raman spectroscopy and ab initio molecular orbital and density functional theories. The products of the reaction are protonated ion of DMAE ($DMAEH^+$), hydrogencarbonate ion, and carbonate ion. The $DMAEH^+$ species in the aqueous solution assumes predominantly the $G^{\mp}G^{\pm}t$ conformation around the $HN^+-C-C-OH$ bonds. $DMAEH^+$ in solid $DMAEH^+Cl^-$ and in acidic aqueous solution also assumes the same conformation. This conformational property of $DMAEH^+$ is contrasted with the results for the DMAE molecules in the liquid state and in aqueous solution that they assume the $G^{\mp}Tx$ ($x$ = t, $g^{\mp}$, or $g^{\pm}$) and $G^{\mp}G^{\pm}g^{\mp}$ conformations around the $LN-C-C-OH$ bonds (L, lone pair). The $G^{\mp}G^{\pm}t$ conformation of $DMAEH^+$ is stabilized by strong intramolecular 1,4-$NH^+\cdots O$ hydrogen bonding, while the $G^{\mp}Tx$ and $G^{\mp}G^{\pm}g^{\mp}$ conformations of DMAE are made stable through the competition of intermolecular hydrogen bonding and intramolecular 1,4-$OH\cdots N$ hydrogen bonding. The interconversion, depending on the acidity/basicity of the environment, of strong $NH^+\cdots O$ hydrogen bonding and $OH\cdots N$ hydrogen bonding or $N\cdots O$ repulsion is certainly one of the important structural factors in chemical and biological reaction processes.

## Introduction

For the purpose of preventing global warming, there is a growing interest in the methods for removing carbon dioxide from natural and refinery gases. The carbon dioxide ($CO_2$) recovery by amino alcohols is one of the promising methods, and the interactions between amino compounds and $CO_2$ have in fact been studied extensively by experimental and theoretical methods.[1−8] The chemical species in aqueous amino alcohol solutions with $CO_2$ dissolved have been identified by NMR and Raman spectroscopies.[1,9] Conformational behavior of the relevant chemical species is important for characterizing their physical, chemical, and biological properties. Infrared and Raman spectroscopy is a powerful technique for analyzing conformational behavior of molecules involved in the reaction system.

2-(*N*,*N*-Dimethylamino)ethanol (DMAE), $(CH_3)_2NCH_2CH_2OH$, is known as one of the model compounds of reversible $CO_2$ absorbents.[1,4,6] Microwave spectroscopy has shown that DMAE and its related compound, 2-aminoethanol ($NH_2CH_2CH_2OH$), assume in the gaseous state the gauche$^{\mp}$−gauche$^{\pm}$−gauche$^{\mp}$ ($G^{\mp}G^{\pm}g^{\mp}$) conformation around the $LN-C-C-OH$ bonds, where L denotes the lone pair, and this conformation is stabilized by intramolecular hydrogen bonding between the amino and hydroxyl groups.[10,11] Matrix-isolation infrared spectroscopy and ab initio molecular orbital and density functional theories have shown that the relevant intramolecular interactions involved play an important role in the conformational stabilization of $XCH_2CH_2OH$-type molecules, where X = $CH_3CH_2$, $CH_3O$, $CH_3S$, and $NH_2$,[12−15] and $(CH_3)_2NCH_2CH_2CH_3$.[16] While the conformational stability of isolated molecules in the gas phase or in matrix is determined by the relevant intramolecular interactions, the conformational stability of molecules in the condensed phases, such as the species in the $DMAE-CO_2-H_2O$ reaction system, is determined in many cases by the competition of the relevant intermolecular and intramolecular interactions.

In the present work, we have studied by infrared and Raman spectroscopy and ab initio molecular orbital and density functional theories the reaction process of the $DMAE-CO_2-H_2O$ system and the conformation of the chemical species present in the system. In order to discuss comparatively, we have also studied the conformation of isolated DMAE molecules in an argon matrix and of molecules in the solid and liquid states and in aqueous solution.

S1089-5639(98)02562-6 CCC: $15.00 
Published on Web 09/22/1998

## Experimental Section

DMAE was supplied by Tokyo Kasei Kogyo and was dried with calcium hydride. Matrix-isolation infrared spectra of DMAE were measured by spraying premixed gas of Ar/DMAE = 1200 to deposit onto a cesium iodide plate cooled to 11 K by an Iwatani CryoMini D105 refrigerator. To study the effect of annealing, the deposited sample was kept at different constant temperatures, increasing from 11 to 40 K, for 10 min each time and was then cooled to 11 K to record the spectra. The infrared spectra were recorded on a JEOL JIR-40X Fourier transform spectrophotometer using a TGS detector by co-addition of 100 scans at a resolution of 1 $cm^{-1}$.

The Raman spectra of DMAE were measured for the solid and liquid states and for aqueous solutions. The spectra for the solid state at 77 K and the liquid state at 190 K were measured on the sample contained in a sealed ampule placed on a copper block cooled with liquid nitrogen. The spectra of the liquid without $CO_2$ and that saturated with $CO_2$ were measured at 298 K under a pressure of 300 kPa, and the spectra of aqueous solution of 30% concentration without $CO_2$ and that saturated with $CO_2$ were measured at 298 K under atmospheric pressure. Raman spectra were also measured on hydrochloric acid solutions of DMAE and on solid dimethyl-2-hydroxyethylammonium chloride, $[(CH_3)_2NHCH_2CH_2OH]^+Cl^-$ or $DMAEH^+Cl^-$, prepared by a reaction of DMAE with hydrogen chloride. The Raman spectra were recorded on a JEOL JRS-400D spectrophotometer equipped with a Hamamatsu R649 photomultiplier by using the 514.5 nm line of an NEC GLG3200 argon ion laser for excitation.

## Calculations

Ab initio calculations were performed on all of the 14 possible conformers of DMAE and seven conformers out of the 14 possible conformers of protonated ion of DMAE ($DMAEH^+$) by the restricted Hartree−Fock method using the 6-31G** basis set (HF/6-31G**) and on several of more stable conformers of DMAE and $DMAEH^+$ by the second-order Møller−Plesset perturbation theory using the 6-31G* basis set (MP2/6-31G*) and by density functional theory of B3LYP using the 6-311+G* basis set (B3LYP/6-311+G*). The energies, molecular geometries, and harmonic vibrational wavenumbers[17] were calculated by these methods. The wavenumbers calculated by the HF/6-31G**, MP2/6-31G*, and B3LYP/6-311+G* methods were scaled by factors 0.91, 0.95, and 1.00, respectively, for the vibrations above 600 $cm^{-1}$ and by factors 0.94, 0.98, and 1.00, respectively, for the vibrations below 600 $cm^{-1}$.[19] The calculations were carried out with the GAUSSIAN 94 program[20] using the default parameters.

## Results and Discussion

Prior to discussing the conformational properties of the chemical species in the DMAE−$CO_2$−$H_2O$ reaction system, we will describe the conformational stabilities of isolated molecules of DMAE and protonated ion of DMAE ($DMAEH^+$) and the relevant interactions involved on the basis of the results of ab initio calculations and matrix-isolation infrared spectroscopy and will subsequently discuss the conformational stabilities of DMAE and $DMAEH^+$ in the condensed phases in the light of the Raman spectroscopic observations.

**Conformational Stabilities of DMAE and $DMAEH^+$.** The relative energies of the conformers of DMAE and $DMAEH^+$ calculated by the HF/6-31G**, MP2/6-31G*, and B3LYP/6-311+G* methods are given in Table 1. The molecular structures of three typical conformers of DMAE and $DMAEH^+$ are depicted in Figure 1. The conformations of DMAE and $DMAEH^+$ are designated by T or t for trans and $G^{\pm}$ or $g^{\pm}$ for gauche$^{\pm}$ around the sequence of bonds LN−C−C−OH and $HN^+$−C−C−OH, respectively, where L denotes the lone pair on nitrogen and the lowercase letters apply to the conformation around the CC−OH bond.

**TABLE 1: Relative Energies of Conformers of DMAE and $DMAEH^+$ Calculated by Different ab Initio Methods**

| | relative energy/kJ $mol^{-1}$ | | | |
|---|---|---|---|---|
| conformer | HF/ 6-31G** | MP2/ 6-31G* | B3LYP/ 6-311+G* | interaction involved[a] |
| | DMAE, $(CH_3)_2N-CH_2-CH_2-OH$ | | | |
| $G^{\mp}G^{\pm}g^{\mp}$ | 0.0 | 0.0 | 0.0 | OH···N |
| $G^{\mp}Tt$ | 11.8 | 20.4 | 14.2 | |
| $G^{\mp}Tg^{\mp}$ | 12.3 | | | |
| $G^{\mp}Tg^{\pm}$ | 12.6 | | | |
| $G^{\mp}G^{\mp}t$ | 13.7 | 18.0 | | CH···O |
| $G^{\mp}G^{\mp}g^{\mp}$ | 13.8 | | | CH···O |
| TTt | 16.8 | | | |
| $TG^{\pm}t$ | 17.0 | 22.2 | | CH···O |
| $TTg^{\pm}$ | 17.5 | | | |
| $TG^{\pm}g^{\pm}$ | 17.8 | | | CH···O |
| $G^{\mp}G^{\pm}t$ | 19.4 | 25.2 | | |
| $TG^{\pm}g^{\mp}$ | 20.1 | | | |
| $G^{\mp}G^{\pm}g^{\pm}$ | *b* | | | |
| $G^{\mp}G^{\mp}g^{\pm}$ | *b* | | | |
| | $DMAEH^+$, $(CH_3)_2NH^+-CH_2-CH_2-OH$[c] | | | |
| $G^{\mp}G^{\pm}t$ | 0.0 | 0.0 | 0.0 | $NH^+$···O |
| $TG^{\pm}t$ | 17.7 | 17.8 | 18.0 | CH···O |
| $G^{\mp}Tt$ | 33.8 | 39.9 | 34.8 | |
| TTt | 38.9 | | | |
| $G^{\mp}G^{\mp}t$ | *d* | | | CH···O |
| $G^{\mp}G^{\pm}g^{\pm}$ | *d* | | | $NH^+$···O |
| $G^{\mp}G^{\pm}g^{\mp}$ | *d* | | | |

[a] OH···N, intramolecular 1,4-OH···N hydrogen bonding; CH···O, intramolecular 1,5-CH···O interaction; $NH^+$···O, intramolecular 1,4-$NH^+$···O hydrogen bonding. [b] Transformed into $G^{\mp}G^{\pm}g^{\mp}$ during structure optimization. [c] For $TG^{\pm}x$, $G^{\mp}Tx$, TT*x*, and $G^{\mp}G^{\mp}x$, structures of only those conformers with the trans conformation around the CC−OH bond ($x$ = t) were optimized. [d] Transformed into $G^{\mp}G^{\pm}t$ during structure optimization.

The ab initio calculations showed that the most stable conformer of DMAE is $G^{\mp}G^{\pm}g^{\mp}$, which is exceedingly more stable than others. This conformation is stabilized by intramolecular 1,4-OH···N hydrogen bonding as indicated by the calculated results that the nonbonded OH···N distance is 2.14 Å (MP2/6-31G*), which is considerably shorter than the sum of the van der Waals radii of hydrogen and nitrogen, 2.70 Å, and that the partial charges of the atoms are $O^{-0.76}-H^{+0.46}\cdots N^{-0.59}$ in units of *e*.

The low-energy conformers of DMAE following $G^{\mp}G^{\pm}g^{\mp}$ are $G^{\mp}Tx$ ($x$ = t, $g^{\mp}$, and $g^{\pm}$) and $G^{\mp}G^{\mp}x$ ($x$ = t and $g^{\mp}$). In the $G^{\mp}G^{\mp}t$ and $G^{\mp}G^{\mp}g^{\mp}$ conformers, one of the $CH_3$(N) groups is located close to the oxygen atom. The stability of these conformers is explained by intramolecular 1,5-CH···O interaction, because the nonbonded CH···O distance was calculated to be 2.33 Å (MP2/6-31G*), which is significantly shorter than the sum of the relevant van der Waals radii, 2.60 Å, and the partial charges were calculated as $C^{-0.30}-H^{+0.21}\cdots O^{-0.74}$. This type of attractive intramolecular CH···O interactions has been found for 1,2-dimethoxyethane,[21−23] 2-(methylthio)ethanol,[14] and 1-methoxy-2-(methylthio)ethane.[24] Other conformers of DMAE are not as stable as the above-mentioned conformers owing to anticipated repulsions between the $CH_3$(N) and(C)-$CH_2$(O) groups or between the lone pairs on nitrogen and oxygen.

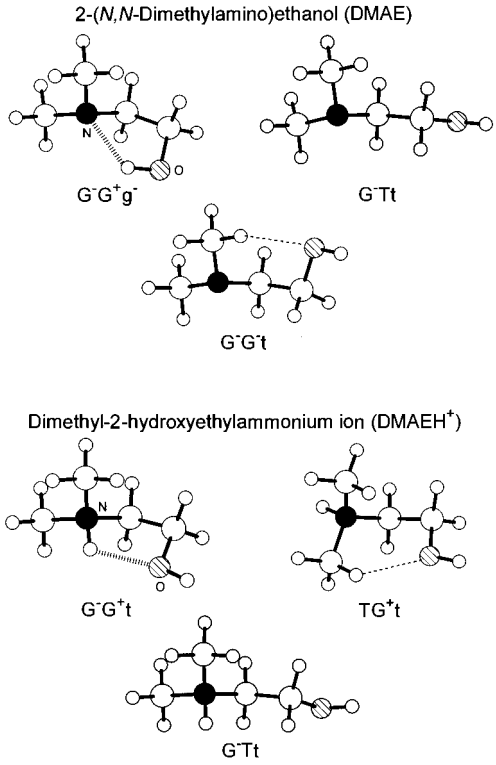


**Figure 1.** Molecular structures of the $G^-G^+g^-$, $G^-Tt$, and $G^-G^-t$ conformers of DMAE and the $G^-G^+t$, $TG^+t$, and $G^-Tt$ conformers of $DMAEH^+$. Stack bars indicate 1,4-OH···N hydrogen bonding for DMAE or 1,4-$NH^+$···O hydrogen bonding for $DMAEH^+$ and a dashed line indicates 1,5-CH···O interaction.

The calculations have shown that the most stable conformer of $DMAEH^+$ is $G^{\mp}G^{\pm}t$, which is far more stable than others. The high stability of this conformation is explained by strong intramolecular 1,4-$NH^+$···O hydrogen bonding as supported by the calculated nonbonded $NH^+$···O distance 2.02 Å (MP2/6-31G*), which is much shorter than the sum of the van der Waals radii of hydrogen and oxygen, 2.60 Å, and the calculated partial charges $N^{-0.67}-H^{+0.49}\cdots O^{-0.78}$. The second most stable conformer $TG^{\pm}t$ is stabilized most probably by intramolecular 1,5-CH···O interaction in conformity with the calculated nonbonded CH···O distance 2.23 Å and the partial charges $C^{-0.36}-H^{+0.29}\cdots O^{-0.75}$.

**Matrix-Isolation Infrared Spectra of DMAE.** Figure 2 shows the infrared spectra of DMAE in an argon matrix with Ar/DMAE = 1200 and the spectra calculated by the MP2/6-31G* method for the $G^{\mp}G^{\pm}g^{\mp}$, $G^{\mp}Tt$, and $G^{\mp}G^{\mp}t$ conformers. The observed wavenumbers of DMAE in the matrix-isolated state and in other phases and the calculated wavenumbers are given in Table 2. The conformational equilibration of matrix-isolated DMAE molecules was monitored by annealing the sample, because the annealing process induces a transformation of less stable conformations into the most stable conformation.[25,26] On annealing at 40 K, the weak bands at 1033, 1040, 1075, 1156, and 1287 $cm^{-1}$, as marked with an arrow in Figure 2a, decrease in relative intensity. The bands which persist in the spectrum after annealing (Figure 2b) coincide with the calculated bands of the most stable $G^{\mp}G^{\pm}g^{\mp}$ conformer (Figure 2c), while the above-mentioned bands whose intensities decrease on annealing match the calculated bands of the $G^{\mp}Tt$ conformer (Figure 2d). Since the relative energies and the vibrational wavenumbers of the $G^{\mp}Tt$, $G^{\mp}Tg^{\mp}$, and $G^{\mp}Tg^{\pm}$ conformers are similar among them, these decreasing bands are assignable to these conformers. The spectral observations mentioned above

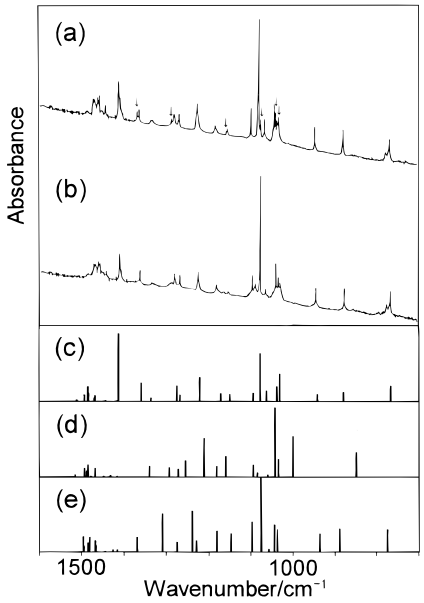


**Figure 2.** Infrared spectra of DMAE in an argon matrix measured (a) immediately after the sample deposition at 11 K and (b) after annealing at 40 K for 10 min, and the spectra calculated by the MP2/6-31G* method for (c) $G^{\mp}G^{\pm}g^{\mp}$, (d) $G^{\mp}Tt$, and (e) $G^{\mp}G^{\mp}t$ conformers. The bands which decrease in relative intensity on annealing are marked with an arrow in (a).

show that the most stable conformer of DMAE in an argon matrix is $G^{\mp}G^{\pm}g^{\mp}$, being consistent with the results for the gas phase by microwave spectroscopy[10] and with the results of ab initio calculations (Table 1).

The predominant existence of the $G^{\mp}G^{\pm}g^{\mp}$ conformer in the matrix is also confirmed by examining the O−H stretching region of the spectra. In this region, only a single band is observed at 3498 $cm^{-1}$, which is assigned to intramolecular hydrogen-bonded species, because free O−H stretching bands are observed at higher wavenumber of about 3660 $cm^{-1}$ in most cases.[12,27] In consideration of the results of the MP2/6-31G* calculations that the O−H stretching wavenumber of the $G^{\mp}G^{\pm}g^{\mp}$ conformer with intramolecular hydrogen bonding is 3473 $cm^{-1}$ and the wavenumber of the $G^{\mp}Tt$ conformer with a free O−H bond is 3594 $cm^{-1}$, the band observed at 3498 $cm^{-1}$ in the matrix is assigned reasonably to the $G^{\mp}G^{\pm}g^{\mp}$ conformer, for which the formation of an intramolecular 1,4-OH···N hydrogen bond is possible.

**Raman Spectra of DMAE in the Condensed Phases.** The Raman spectra of DMAE in the solid and liquid states and 30% aqueous solution of DMAE are shown in Figure 3, where the calculated spectra of six more stable conformers, $G^{\mp}G^{\pm}g^{\mp}$, $G^{\mp}Tt$, $G^{\mp}Tg^{\mp}$, $G^{\mp}Tg^{\pm}$, $G^{\mp}G^{\mp}t$, and $G^{\mp}G^{\mp}g^{\mp}$, are also shown. The Raman spectrum of the solid state in the 300−1000 $cm^{-1}$ region (Figure 3a) exhibits fewer number of bands than the spectra of other condensed phases. A comparison of the solid-state spectrum with the calculated results shows that it matches closely the calculated spectra of the $G^{\mp}Tx$ conformers, where *x* is t, $g^{\mp}$, or $g^{\pm}$ (Figure 3f−h). This provides evidence that the conformation of DMAE molecules in the solid state is $G^{\mp}Tx$.

The spectra of DMAE in the liquid state and in aqueous solution (Figure 3b−d) show a number of bands that correspond to the bands in the spectrum of the solid state, e.g. those at 492 and 851 $cm^{-1}$. The Raman spectra of these condensed phases also show several bands, such as those at 548, 776, and 943 $cm^{-1}$, which have their counterparts in the matrix-isolation infrared spectra (Figure 2) but are missing in the solid-state spectrum. These spectral observations indicate that DMAE

**TABLE 2: Observed and Calculated Vibrational Wavenumbers[a] ($cm^{-1}$) of DMAE**

| infrared[b] | | | Raman[b] | | | HF/6-31G**[c,d] | | | | | | MP2/6-31G*[c] | |
|---|---|---|---|---|---|---|---|---|---|---|---|---|---|
| matrix (11 K) | matrix (40 K) | liquid (298 K) | solid (77 K) | liquid (298 K) | aq soln (298 K) | $G^{\mp}G^{\pm}g^{\mp}$ | $G^{\mp}Tt$ | $G^{\mp}Tg^{\mp}$ | $G^{\mp}Tg^{\pm}$ | $G^{\mp}G^{\mp}t$ | $G^{\mp}G^{\mp}g^{\mp}$ | $G^{\mp}G^{\pm}g^{\mp}$ | $G^{\mp}Tt$ |
| 1486 vw | 1486 vw | | 1485 m | | | 1513(0.9,10) | 1519(5,8) | 1507(1,4) | 1506(2,5) | 1505(8,11) | 1502(11,10) | 1512 | 1515 |
| 1472 m | 1472 m | | 1475 m | | 1472 vs | 1498(8,16) | 1498(6,24) | 1498(7,23) | 1498(6,22) | 1500(8,17) | 1493(5,28) | 1493 | 1494 |
| 1470 m | 1470 m | | | | | 1492(11,4) | 1497(4,8) | 1494(4,11) | 1494(3,13) | 1491(8,5) | 1490(8,6) | 1485 | 1488 |
| 1468 m | 1468 m | | | | | 1489(11,14) | 1488(12,11) | 1489(14,13) | 1488(13,11) | 1489(6,14) | 1488(3,5) | 1483 | 1485 |
| 1461 m | 1461 m | 1462 s | 1460 vs | 1467 vs | 1467 sh,s | 1481(1,3) | 1484(2,2) | 1482(2,3) | 1483(2,3) | 1481(3,4) | 1481(4,3) | 1470 | 1476 |
| 1457 m | 1457 m | | 1454 s | 1448 s | 1448 vs | 1474(8,27) | 1474(5,25) | 1474(7,22) | 1474(7,23) | 1474(7,22) | 1474(8,20) | 1468 | 1469 |
| 1443 mw | 1443 mw | | 1442 w | | | 1462(2,7) | 1472(2,2) | 1469(1,8) | 1468(1,7) | 1465(2,4) | 1464(0.5,8) | 1443 | 1448 |
| | | | | 1432 sh,m | 1434 sh,m | | 1461(2,6) | | | 1458(2,5) | | | 1431 |
| 1412 ms | 1412 ms | | 1415 mw | | 1414 w | 1439(26,4) | | 1442(5,3) | 1440(4,4) | 1439(6,7) | 1439(6,7) | 1417 | |
| 1407 m | 1407 m | 1408 w | | 1406 ms | | 1438(39,5) | 1439(5,7) | | | | 1426(17,2) | 1413 | 1416 |
| 1368 mw | | | | | | | | 1436(3,6) | 1435(3,4) | | | | |
| 1364 mw | 1364 m | 1365 m | | 1366 vw | 1372 vw | 1396(40,2) | | | | 1406(22,2) | 1402(42,2) | 1359 | |
| 1335 w | 1335 w | | 1333 vw | | 1333 vw | 1357(12,11) | 1378(20,0.7) | 1385(55,3) | | | 1370(21,8) | 1336 | 1340 |
| 1333 w | | 1328 w | | 1325 vw | | | | | 1370(79,3) | | | | |
| 1287 w | 1290 vw | | 1303 s | 1301 mw | 1310 mw | | 1320(14,10) | 1342(5,8) | 1351(13,2) | 1340(40,10) | 1331(21,7) | | 1293 |
| 1281 mw | 1281 m | | | | 1298 sh,vw | 1311(29,3) | | | 1321(15,12) | | | 1275 | |
| 1271 w | | | 1270 vw | 1270 w | 1263 sh,vw | | 1306(18,0.8) | 1313(16,6) | | | | | 1272 |
| 1269 mw | 1268 m | 1269 ms | 1253 vw | 1248 w | 1253 w | 1301(13,0.8) | | 1305(20,1) | 1306(21,0.2) | 1306(12,1) | 1307(8,1) | 1268 | |
| | | 1247 m | 1242 vw | | | | 1283(14,9) | 1269(22,4) | | 1263(7,6) | | | 1254 |
| 1226 ms | 1226 ms | 1225 sh,w | | | | 1240(40,6) | | | 1260(11,3) | 1261(49,4) | | 1222 | |
| 1224 m | | | | | | | 1228(64,4) | | | | 1222(29,6) | | 1211 |
| 1182 w | 1183 mw | 1180 m | 1186 mw | 1178 w | 1176 sh,w | 1188(13,4) | 1203(23,1) | 1188(12,2) | 1191(19,3) | 1199(30,3) | 1208(26,2) | 1171 | 1181 |
| 1156 w | | 1157 m | 1168 w | 1157 m | 1167 mw | | 1178(40,1) | | | 1163(27,3) | 1153(32,3) | | 1159 |
| 1154 w | 1155 w | | | | | 1170(10,3) | | 1135(56,2) | 1140(5,3) | | | 1150 | |
| 1098 ms | 1098 ms | 1100 s | 1110 w | 1099 w | 1104 w | 1112(95,4) | 1109(14,4) | 1107(6,4) | 1108(10,5) | 1111(37,6) | 1112(25,7) | 1094 | 1095 |
| | 1094 w | | | | | | | | | | | | |
| | 1091 w | | 1090 w | | | 1108(16,5) | 1092(8,3) | | | 1099(61,1) | 1099(36,3) | 1077 | 1084 |
| 1082 s | | | 1081 w | 1081 w | 1085 w | | | 1088(79,10) | 1088(70,11) | | | | |
| 1080 vs | 1080 vs | 1086 s | | | | 1073(11,1) | | | | | | 1063 | |
| 1075 m | | | | | | | 1085(66,10) | | | | | | 1059 |
| 1066 m | 1066 mw | | 1065 vs | 1065 m | 1066 m | | | 1073(2,4) | 1061(26,5) | 1071(2,3) | 1066(23,7) | | |
| | | | 1054 m | | | | | | 1055(53,2) | 1057(16,8) | | | |
| 1043 s | 1043 s | 1041 vs | 1050 m | 1044 s | 1040 s | 1050(27,6) | 1057(45,5) | 1051(36,7) | | | 1051(33,7) | 1038 | 1043 |
| 1040 ms | | | 1041 s | | | | 1049(22,7) | 1048(74,6) | 1046(76,7) | 1049(36,10) | | | 1035 |
| 1037 m | 1037 ms | | | | 1034 sh,s | 1043(40,8) | | | | | | 1031 | |
| 1033 ms | 1033 m | | 1024 m | 1026 sh,m | 1022 m | | 993(30,7) | 1015(11,3) | 1014(9,4) | | 1026(34,3) | | 999 |
| 948 ms | 948 ms | 945 ms | | 945 mw | 943 mw | 943(12,5) | | | | 941(17,4) | 944(28,5) | 941 | |
| 882 w | | 895 w | | | | | | | | 901(15,1) | 897(15,1) | | |
| 881 ms | 881 ms | 876 m | 868 mw | 876 m | 874 m | 878(9,7) | | | | | | 879 | |
| | | 857 m | 853 s | 857 m | 851 m | | 855(24,10) | | 855(17,9) | | | | 849 |
| | | | | 852 sh,m | | | | 854(17,9) | | | | | |
| | | | 812 mw | | | | 796(0.3,0.4) | | | | | | 801 |
| 780 w | 781 w | | 781 vw | | | | | 782(3,0.2) | 781(1,0.3) | | | | |
| 771 ms | 771 ms | 776 ms | | 778 vs | 776 vs | 768(22,11) | | | | | | 767 | |
| | | | | 762 sh,w | 762 sh,w | | | | | 775(18,14) | 768(13,13) | | |
| 563 w | 562 w | | | 548 w | 548 w | 560(8,2) | | | | | | 573 | |
| | | | | 535 w | 535 w | | | | | 527(8,1) | 539(21,1) | | |
| | | 491 w | 508 s | 494 m | 492 m | | 501(2,2) | 503(3,3) | 502(3,3) | | | | 499 |
| 475 m | 475 m | | | | | 469(112,2) | | | | | | 551 | |
| | | | 454 ms | 440 m | 451 m | 433(13,0.4) | 434(4,1) | 436(7,1) | 435(4,1) | 439(2,0.2) | 441(0.3,0.1) | 435 | 434 |
| | | | | | 443 sh,m | | | | | | | | |
| | | | 418 m | 412 br,w | 422 m | 414(6,0.4) | 396(12,0.4) | 394(19,0.4) | 395(21,0.3) | 385(9,0.8) | 381(7,1) | 413 | 402 |
| | | | 375 s | 366 s | 369 s | 364(13,0.6) | 362(3,1) | 365(5,2) | 363(4,2) | 341(4,0.6) | 344(17,0.8) | 379 | 362 |
| | | | 303 w | | | | | 302(142,3) | 295(141,2) | 290(18,0.7) | 315(121,2) | | |
| | | | 281 mw | | | 283(0.2,0.1) | 266(4,0.4) | | | | | 296 | 276 |
| | | | 272 vw | 260 br,w | | | 260(139,4) | 263(0.5,0.3) | 264(4,0.5) | 263(102,3) | 272(22,0.8) | | 270 |
| | | | | | | 248(0.5,0.4) | | | | 244(7,0.7) | 254(8,0.5) | 260 | |
| | | | 234 w | | | 232(0.4,0.3) | 232(2,0.1) | 233(2,0.3) | 233(0.5,0.3) | 233(18,0.1) | 234(8,0.4) | 238 | 247 |
| | | | 195 w | | | | 200(4,0.1) | 198(0.7,0.2) | 200(0.1,0.2) | | | | 200 |
| | | | 151 w | | | 138(4,0.1) | | | | 154(8,0.1) | 151(2,0.3) | 149 | |
| | | | 138 w | | | | | | | | | | |
| | | | 108 ms | | | | 111(0.6,0.1) | 116(3,0.1) | 113(2,0.1) | | | | 115 |
| | | | 84 w | | | 66(2,0.2) | 63(12,0.2) | 59(6,0.1) | 68(3,0.3) | 45(2,0.1) | 61(2,0.1) | 62 | 48 |

[a] Wavenumbers below 1500 $cm^{-1}$ are given in this table. [b] Approximate relative intensities: vs, very strong; s, strong; ms, medium strong; m, medium; mw, medium weak; w, weak; vw, very weak; sh, shoulder; br, broad. [c] For scale factors, see text. [d] Infrared intensities in km $mol^{-1}$ and Raman intensities in $Å^4$ $amu^{-1}$ are given in parentheses in this order.

molecules in the liquid state and in aqueous solution assume the $G^{\mp}Tx$ ($x$ = t, $g^{\mp}$, or $g^{\pm}$) and $G^{\mp}G^{\pm}g^{\mp}$ conformations. Of these, the $G^{\mp}G^{\pm}g^{\mp}$ conformer is one of the major conformers in these condensed phases, because the band at 776 $cm^{-1}$ is distinctively strong as compared with other bands. The relative intensities of the Raman bands at 492 and 851 $cm^{-1}$ associated with the $G^{\mp}Tx$ conformers are stronger in the liquid state at 190 K than at 298 K. This spectral behavior indicates that the $G^{\mp}Tx$ conformers are more stable than the $G^{\mp}G^{\pm}g^{\mp}$ conformer. In addition to these conformers, the $G^{\mp}G^{\mp}x$ conformers are also present in the liquid state and in aqueous solution as indicated by an observation of a weak band at 762 $cm^{-1}$ associated with these conformers.

In the condensed phases, intermolecular interactions such as OH···O and OH···N hydrogen bonding are more important than intramolecular interactions, and may stabilize the $G^{\mp}Tx$ con-

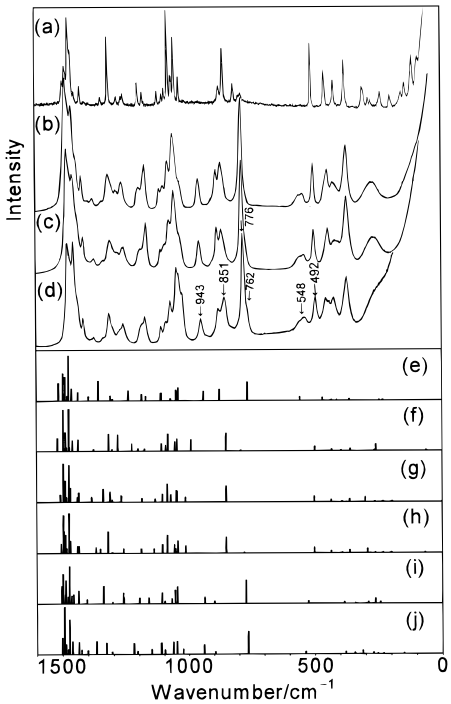


**Figure 3.** Raman spectra of DMAE in (a) the solid state at 77 K, (b) the liquid state at 190 K, (c) the liquid state at 298 K, and (d) 30% aqueous solution at 298 K, and the spectra calculated by the HF/6-31G** method for (e) $G^{\mp}G^{\pm}g^{\mp}$, (f) $G^{\mp}Tt$, (g) $G^{\mp}Tg^{\mp}$, (h) $G^{\mp}Tg^{\pm}$, (i) $G^{\mp}G^{\mp}t$, and (j) $G^{\mp}G^{\mp}g^{\mp}$ conformers.

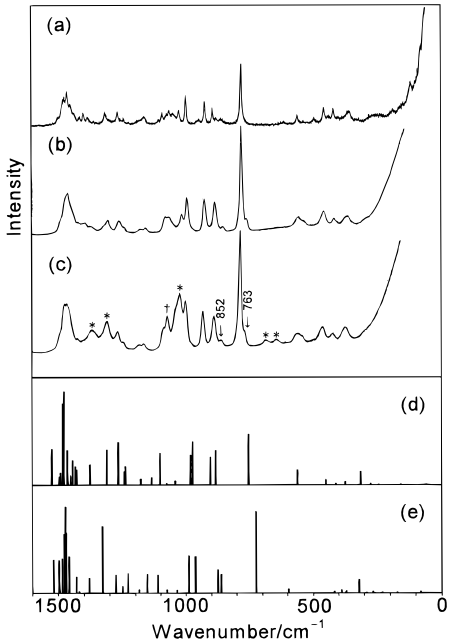


**Figure 4.** Raman spectra at 298 K of (a) $DMAEH^+Cl^-$ in the solid state, (b) hydrochloric acid solution of DMAE, and (c) 30% aqueous solution of DMAE saturated with $CO_2$, and the spectra calculated by the HF/6-31G** method for (d) $G^{\mp}G^{\pm}t$ and (e) $TG^{\pm}t$ conformers. The bands due to hydrogencarbonate and carbonate ions are marked with an asterisk and a dagger, respectively, in (c).

formers to a greater extent than the $G^{\mp}G^{\pm}g^{\mp}$ conformer which is stabilized by intramolecular 1,4-OH···N hydrogen bonding. The energy of the intermolecular hydrogen bonding may precede the thermal energy in the condensed phases at low temperatures.

**Raman Spectra of $DMAEH^+$ and a Reaction of Aqueous DMAE Solutions with $CO_2$.** Figure 4 shows the Raman spectra of dimethyl-2-hydroxyethylammonium chloride ($DMAEH^+Cl^-$) in the solid state, hydrochloric acid solution of DMAE, and 30% aqueous solution of DMAE saturated with $CO_2$. The calculated spectra of the most stable two conformers of $DMAEH^+$, $G^{\mp}G^{\pm}t$ and $TG^{\pm}t$, are also shown in this figure. The observed and calculated wavenumbers of $DMAEH^+$ are given in Table 3. A comparison of the spectrum of solid $DMAEH^+Cl^-$ (Figure 4a) with the calculated spectra indicates that $DMAEH^+$ molecules assume the $G^{\mp}G^{\pm}t$ conformation. The spectrum of hydrochloric acid solution of DMAE (Figure 4b) is similar to the spectrum of solid $DMAEH^+Cl^-$. This observation shows that DMAE molecules in hydrochloric acid solution are protonated as $DMAEH^+$ assuming the conformation mostly of $G^{\mp}G^{\pm}t$.

The Raman spectrum of 30% aqueous solution of DMAE saturated with $CO_2$ (Figure 4c) is substantially the same as the spectrum of hydrochloric acid solution of DMAE except for several additional bands in the former spectrum at 636, 678, 1018, 1301, and 1362 cm$^{-1}$ due to hydrogencarbonate ion ($HCO_3^-$) and at 1065 cm$^{-1}$ due to carbonate ion ($CO_3^{2-}$).[28] These spectral features indicate that DMAE acts as a Lewis base in a hydration reaction of $CO_2$ in aqueous solution:

$$(CH_3)_2NCH_2CH_2OH + CO_2 + H_2O \rightarrow (CH_3)_2NH^+CH_2CH_2OH + HCO_3^-$$

This elucidation of the reaction of aqueous DMAE solutions with $CO_2$ is consistent with the interpretation by NMR spectroscopy.[1] The Raman spectrum of neat liquid of DMAE, on the other hand, showed no noticeable changes on saturation with $CO_2$ under a pressure of 300 kPa except for the appearance of a very weak band of $CO_2$ at 1383 cm$^{-1}$. This spectral behavior indicates that a reaction of DMAE with $CO_2$ does not occur in the absence of water.

The spectral coincidence of the $DMAEH^+$ species in the DMAE−$CO_2$−$H_2O$ reaction system with the same species in hydrochloric acid solution of DMAE confirms that $DMAEH^+$ assumes predominantly the $G^{\mp}G^{\pm}t$ conformation in either of the solutions. In addition to this major conformation, $DMAEH^+$ also assumes the $TG^{\pm}t$ conformation as indicated by an observation of weak bands at 763 and 852 cm$^{-1}$ associated with this conformation.

**Intramolecular 1,4-$NH^+$···O and 1,4-OH···N Hydrogen Bonding.** To study more closely the conformational stabilization of DMAE and $DMAEH^+$ molecules by intramolecular 1,4-$NH^+$···O and 1,4-OH···N hydrogen bonding, we have performed higher-level density functional calculations by the B3LYP/6-311+G* method. According to the calculated results (Table 1), the $G^{\mp}G^{\pm}t$ conformer of $DMAEH^+$ with 1,4-$NH^+$···O hydrogen bonding involved is more stable than the $G^{\mp}Tt$ conformer with the least steric repulsions by 34.8 kJ mol$^{-1}$, while the $G^{\mp}G^{\pm}g^{\mp}$ conformer of DMAE with 1,4-OH···N hydrogen bonding involved is more stable than the $G^{\mp}Tt$ conformer by 14.2 kJ mol$^{-1}$. The calculations by the HF/6-31G** and MP2/6-31G* methods also gave similar tendencies of the relative energies of the conformers. These calculated results imply that 1,4-$NH^+$···O hydrogen bonding is stronger more than twice than 1,4-OH···N hydrogen bonding, and is strong enough to maintain the $G^{\mp}G^{\pm}t$ conformation in the condensed phases. Strong hydrogen bonding, in which ions are involved, has been reported on FH···$F^-$, OH···$O^-$, and $O^+$H···O.[29−31]

The present study has shown that intermolecular OH···O or OH···N hydrogen bonding is stronger than intramolecular 1,4-OH···N hydrogen bonding and that the major conformers of DMAE present in the liquid state and in aqueous solution are

**TABLE 3: Observed and Calculated Vibrational Wavenumbers[a] ($cm^{-1}$) of $DMAEH^+$**

| Raman[b] | | | HF/6-31G**[c,d] | | MP2/6-31G*[c] | | B3LYP/6-311+G*[c] |
|---|---|---|---|---|---|---|---|
| solid | HCl aq soln | $CO_2$ aq soln | $G^{\mp}G^{\pm}t$ | $TG^{\pm}t$ | $G^{\mp}G^{\pm}t$ | $TG^{\pm}t$ | $G^{\mp}G^{\pm}t$ |
| 1472 br,ms | 1483 sh,w | 1484 sh,mw | 1525(6) | 1520(6) | 1519 | 1514 | 1544 |
| | | | 1497(1) | 1498(6) | 1489 | 1493 | 1527 |
| | | | 1491(2) | 1497(0.8) | 1480 | 1488 | 1521 |
| 1461 s | 1464 sh,ms | 1468 ms | 1484(15) | 1485(6) | 1476 | 1474 | 1518 |
| 1448 ms | 1458 ms | 1458 ms | 1478(25) | 1477(11) | 1469 | 1468 | 1507 |
| | | | 1461(1) | 1473(16) | 1455 | 1460 | 1494 |
| 1432 m | 1448 sh,m | 1442 sh,mw | 1465(6) | 1471(11) | 1433 | 1444 | 1485 |
| 1409 w | 1418 vw | 1418 w | 1452(2) | 1460(7) | 1418 | 1440 | 1477 |
| | | | 1445(4) | 1431(3) | 1426 | 1410 | 1457 |
| 1394 m | 1392 w | | 1434(3) | 1431(1) | 1412 | 1396 | 1455 |
| 1378 mw | 1368 vw | 1362 br,mw[e] | 1429(3) | 1421(0.2) | 1393 | 1392 | 1448 |
| 1308 m | 1313 sh,w | | 1378(4) | 1380(3) | 1342 | 1352 | 1397 |
| | 1301 mw | 1301 m[e] | 1310(6) | 1330(12) | 1289 | 1310 | 1334 |
| 1260 m | 1256 mw | 1261 mw | 1266(8) | 1277(3) | 1239 | 1251 | 1280 |
| | | | 1244(2) | 1250(1) | 1224 | 1231 | 1257 |
| 1236 vw | 1237 w | 1239 w | 1237(3) | 1229(4) | 1213 | 1205 | 1252 |
| 1174 br,vw | 1172 vw | 1178 w | | 1186(0.6) | | 1167 | |
| 1158 w | 1154 w | 1158 w | 1178(1) | | 1157 | | 1188 |
| | | | 1137(1) | 1155(3) | 1123 | 1142 | 1158 |
| 1085 mw | 1075 mw | 1078 sh,m | 1078(0.3) | 1078(0.6) | 1061 | 1060 | 1092 |
| 1058 m | 1063 mw | 1065 ms[f] | 1102(6) | 1113(3) | 1063 | 1078 | 1077 |
| 1042 mw | | 1032 sh,ms | | | | | |
| 1019 m | 1013 mw | 1018 s[e] | 1042(0.7) | 1038(0.5) | 1028 | 1023 | 1066 |
| 994 s | 990 ms | 993 ms | 983(5) | 991(7) | 988 | 995 | 994 |
| 943 w | | | 976(8) | 966(7) | 980 | 971 | 985 |
| 921 ms | 923 ms | 924 ms | 905(5) | | 917 | | 926 |
| 890 m | 882 ms | 882 ms | 884(6) | 876(4) | 877 | 883 | 895 |
| | 851 w | 852 w | | 862(3) | | 854 | |
| 778 vs | 776 vs | 779 vs | 753(9) | | 760 | | 771 |
| | 758 w | 763 w | | 726(15) | | 733 | |
| | | 678 vw[g] | | | | | |
| | | 636 vw[g] | | | | | |
| | | | | 597(0.7) | | 593 | |
| 559 w | 553 w | 554 w | 561(3) | | 560 | | 556 |
| | 538 vw[h] | 540 w[h] | | | | | |
| 493 br,vw | | | | | | | |
| 455 mw | 453 mw | 454 mw | 450(1) | | 453 | | 450 |
| 418 mw | 414 w | 415 w | 410(0.3) | 419(0.2) | 413 | 419 | 403 |
| 364 sh,w | | | | 390(0.5) | | 392 | |
| 355 mw | 363 mw | 366 mw | 373(0.6) | 371(0.4) | 378 | 370 | 378 |
| | | | 313(2) | 323(2) | 312 | 336 | 318 |
| | | | | 292(0.1) | | 310 | |
| | | | 274(0.3) | 268(0.3) | 279 | 279 | 264 |
| 254 br,vw | | | 244(0.1) | 230(0.1) | 246 | 234 | 243 |
| | | | 204(0.1) | | 206 | | 203 |
| 186 w | | | 158(0.1) | 174(0.2) | 171 | 185 | 163 |
| 116 m | | | 60(0.1) | 83(0.3) | 63 | 102 | 69 |

[a] Wavenumbers below 1500 $cm^{-1}$ are given in this table. [b] Raman spectra observed at 298 K. Approximate relative intensities: vs, very strong; s, strong; ms, medium strong; m, medium; mw, medium weak; w, weak; vw, very weak; sh, shoulder; br, broad. [c] For scale factors, see text. [d] Raman intensities in $Å^4$ $amu^{-1}$ are given in parentheses. [e] Also assignable to hydrogencarbonate ion. [f] Also assignable to carbonate ion. [g] Assigned to hydrogencarbonate ion. [h] This band may be assigned to the $G^{\mp}G^{\pm}t$ conformer of the species for which the formation of intermolecular hydrogen bonding is different from that for the species giving a band at 553−554 $cm^{-1}$.

those with the trans and gauche conformations around the NC−CO bond, namely $G^{\mp}Tx$ and $G^{\mp}G^{\pm}g^{\mp}$. These results suggest that the conformational competition of the intermolecular and intramolecular hydrogen bonding makes both the conformers with the trans and gauche conformations around the NC−CO bond stable when nitrogen is not protonated as in the liquid state or in aqueous solution, while intramolecular 1,4-$NH^+\cdots O$ hydrogen bonding, which is stronger than intramolecular 1,4-OH···N hydrogen bonding, stabilizes preferentially the gauche conformation around the same bond when nitrogen is protonated as in acidic solutions.

## Conclusions

In the reaction system of aqueous DMAE solutions with $CO_2$ dissolved, the product chemical species are protonated ion of DMAE ($DMAEH^+$), hydrogencarbonate ion, and carbonate ion. The $DMAEH^+$ species in the aqueous solution assumes predominantly the $G^{\mp}G^{\pm}t$ conformation around the $HN^+-C-C-OH$ bonds. $DMAEH^+$ in solid $DMAEH^+Cl^-$ and in acidic aqueous solution also assumes the same conformation. This conformational property of $DMAEH^+$ is contrasted with the results for the DMAE molecules in the liquid state and in aqueous solution that they assume the $G^{\mp}Tx$ ($x$ = t, $g^{\mp}$, or $g^{\pm}$) and $G^{\mp}G^{\pm}g^{\mp}$ conformations around the LN−C−C−OH bonds (L, lone pair). The $G^{\mp}G^{\pm}t$ conformation of $DMAEH^+$ is stabilized by strong intramolecular 1,4-$NH^+\cdots O$ hydrogen bonding, while the $G^{\mp}Tx$ and $G^{\mp}G^{\pm}g^{\mp}$ conformations of DMAE are made stable through the competition of intermolecular hydrogen bonding and intramolecular 1,4-OH···N hydrogen bonding. The interconversion, depending on the acidity/basicity

of the environment, of strong $NH^+\cdots O$ hydrogen bonding and $OH\cdots N$ hydrogen bonding or $N\cdots O$ repulsion is certainly one of the important structural factors in chemical and biological reaction processes.

## References and Notes

(1) Suda, T.; Iwaki, T.; Mimura, T. *Chem. Lett.* **1996**, 777−778.
(2) Meredith, J. C.; Johnston, K. P.; Seminario, J. M.; Kazarian, S. G.; Eckert, C. A. *J. Phys. Chem.* **1996**, *100*, 10837−10848.
(3) Rinker, E. B.; Ashour, S. S.; Sandall, O. C. *Chem. Eng. Sci.* **1995**, *50*, 755−768.
(4) Hagewiesche, D. P.; Ashour, S. S.; Al-Ghawas, H. A.; Sandall, O. C. *Chem. Eng. Sci.* **1995**, *50*, 1071−1079.
(5) Andrés, J.; Moliner, V.; Krechl, J.; Silla, E. *J. Chem. Soc., Perkin Trans. 2* **1993**, 521−523.
(6) Benitez-Garcia, J.; Ruiz-Ibanez, G.; Al-Ghawas, H. A.; Sandall, O. C. *Chem. Eng. Sci.* **1991**, *46*, 2927−2931.
(7) Crooks, J. E.; Donnellan, J. P. *J. Org. Chem.* **1990**, *55*, 1372−1374.
(8) Chakraborty, A. K.; Bischoff, K. B.; Astarita, G.; Damewood, J. R., Jr. *J. Am. Chem. Soc.* **1988**, *110*, 6947−6954.
(9) Ohno, K.; Matsuura, H.; Iwaki, T.; Suda, T. *Chem. Lett.* **1998**, 531−532.
(10) Penn, R. E.; Birkenmeier, J. A. *J. Mol. Spectrosc.* **1976**, *62*, 416−422.
(11) Penn, R. E.; Olsen, R. J. *J. Mol. Spectrosc.* **1976**, *62*, 423−428.
(12) Ohno, K.; Yoshida, H.; Watanabe, H.; Fujita, T.; Matsuura, H. *J. Phys. Chem.* **1994**, *98*, 6924−6930.
(13) Yoshida, H.; Takikawa, K.; Ohno, K.; Matsuura, H. *J. Mol. Struct.* **1993**, *299*, 141−147.
(14) Yoshida, H.; Harada, T.; Murase, T.; Ohno, K.; Matsuura, H. *J. Phys. Chem.* **1997**, *101*, 1731−1737.
(15) Räsänen, M.; Aspiala, A.; Homanen, L.; Murto, J. *J. Mol. Struct.* **1982**, *96*, 81−100.
(16) Ohno, K.; Tonegawa, A.; Yoshida, H.; Matsuura, H. *J. Mol. Struct.* **1997**, *435*, 219−228.
(17) The term "frequency" has been customarily used in the field of vibrational spectroscopy to indicate the quantity actually given in units of $cm^{-1}$ rather than Hz. We use, in this paper, the appropriate terminology of "wavenumber" for this quantity, following SI usage recommended by IUPAC.[18.]
(18) Mills, I.; Cvitaš, T.; Homann, K.; Kallay, N.; Kuchitsu, K. *Quantities, Units and Symbols in Physical Chemistry*; IUPAC, Blackwell: Oxford, UK, 1988.
(19) Scott, A. P.; Radom, L. *J. Phys. Chem.* **1996**, *100*, 16502−16513.
(20) Frisch, M. J.; Trucks, G. W.; Schlegel, H. B.; Gill, P. M. W.; Johnson, B. G.; Robb, M. A.; Cheeseman, J. R.; Keith, T.; Petersson, G. A.; Montgomery, J. A.; Raghavachari, K.; Al-Laham, M. A.; Zakrzewski, V. G.; Ortiz, J. V.; Foresman, J. B.; Cioslowski, J.; Stefanov, B. B.; Nanayakkara, A.; Challacombe, M.; Peng, C. Y.; Ayala, P. Y.; Chen, W.; Wong, M. W.; Andres, J. L.; Replogle, E. S.; Gomperts, R.; Martin, R. L.; Fox, D. J.; Binkley, J. S.; Defrees, D. J.; Baker, J.; Stewart, J. P.; Head-Gordon, M.; Gonzalez, C.; Pople, J. A. *GAUSSIAN 94*, Revision D.3; Gaussian Inc.: Pittsburgh, PA, 1995.
(21) Yoshida, H.; Tanaka, T.; Matsuura, H. *Chem. Lett.* **1996**, 637−638.
(22) Yoshida, H.; Kaneko, I.; Matsuura, H.; Ogawa, Y.; Tasumi, M. *Chem. Phys. Lett.* **1992**, *196*, 601−606.
(23) Astrup, E. E. *Acta Chem. Scand., Ser. A* **1979**, *33*, 655−664.
(24) Yoshida, H.; Harada, T.; Ohno, K.; Matsuura, H. *Chem. Commun.* **1997**, 2213−2214.
(25) Frei, H.; Pimentel, G. C. *Annu. Rev. Phys. Chem.* **1985**, *36*, 491−524.
(26) Barnes, A. J. *J. Mol. Struct.* **1984**, *113*, 161−174.
(27) Barnes, A. J.; Hallam, H. E. *Trans. Faraday Soc.* **1970**, *66*, 1932−1940.
(28) Palmer, D. A.; van Eldic, R. *Chem. Rev.* **1983**, *83*, 651−731.
(29) Huggins, M. L. *Angew. Chem., Int. Ed. Engl.* **1971**, *10*, 147−152.
(30) Joesten, M. D. *J. Chem. Educ.* **1982**, *59*, 362−366.
(31) Jeffrey, G. A.; Saenger, W. *Hydrogen Bonding in Biological Structures*, 2nd ed.; Springer: Berlin, 1994.